

Phase-separated ferromagnetism in spin-imbalanced Fermi atoms loaded on an optical ladder: a density matrix renormalization group study

M. Okumura,^{1,2,*} S. Yamada,^{3,2} M. Machida,^{3,2} and H. Aoki⁴

¹*Computational Condensed Matter Physics Laboratory, RIEN, Wako, Saitama 351-0198, Japan*

²*CREST(JST), 4-1-8 Honcho, Kawaguchi, Saitama 332-0012, Japan*

³*CCSE, Japan Atomic Energy Agency, Higashi-Ueno, Tokyo 110-0015, Japan*

⁴*Department of Physics, University of Tokyo, Hongo, Tokyo 113-0033, Japan*

(Dated: November 13, 2017)

We consider repulsively-interacting cold fermionic atoms loaded on an optical ladder lattice in a trapping potential. The density-matrix renormalization-group method is used to numerically calculate the ground state for systematically varied values of interaction U and spin imbalance p in the Hubbard model on the ladder. The system exhibits rich structures, where a fully spin-polarized phase, spatially separated from other domains in the trapping potential, appears for large enough U and p . The phase-separated ferromagnetism can be captured as a real-space image of the energy gap between the ferromagnetic and other states arising from a combined effect of Nagaoka's ferromagnetism extended to the ladder and the density dependence of the energy separation between competing states. We also predict how to maximize the ferromagnetic region.

PACS numbers: 03.75.Ss, 67.85.Lm, 71.10.Fd

Why cold atoms on a ladder? — Ultracold atom systems offer ideal opportunities for systematic studies of novel quantum many-body phenomena, since they are not only extremely clean, but also controllable to an unusual degree [1]. Particularly, the inter-atomic interaction tunable with the Feshbach resonance create a unique stage for exploring strongly-correlated systems. If we further turn to cold atoms on optical lattices (OL's) prepared by standing waves from laser beams, they provide an even more versatile playing ground [1, 2]. Among the attractive targets are the metal-insulator transition, d -wave superfluidity, and various magnetisms. Actually, the antiferromagnetism via the superexchange interactions between localized Bose atoms on an optical superlattice [3] and the Mott insulator in fermionic atoms on cubic OL [4, 5] have already been achieved.

Now, one big issue in the field of strongly correlated systems is the itinerant ferromagnetism, which is, despite the long history, still far from fully understood. Cold atom systems, with their tunability, should be an unprecedented place for realizing the itinerant ferromagnetism. While there are many theoretical studies on itinerant magnetism in ultracold atom systems [6–11], Jo *et al.* recently reported that the Stoner instability was observed in an ultracold fermionic atom system without OL [12]. However, it has been pointed out that some factors other than Stoner instability may also be involved [13].

In this Rapid Communication, we study strongly-correlated fermionic atoms with a spin-imbalance loaded on an optical ladder, and propose a way to realize and observe the ferromagnetism originated by the finite hole-density Nagaoka mechanism. One tunability unique to cold atoms is we can control the spin balance, which en-

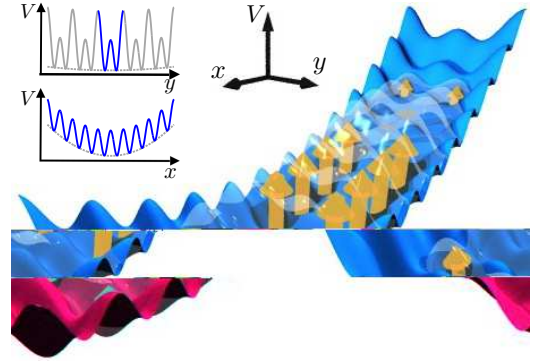


FIG. 1. (Color online) Two-leg ladder optical lattice (corrugated surface in blue) is schematically shown along with the atomic wavefunction (pale cloud) and spins (arrows). Inset depicts simple lattice (along x) and superlattice (y) potentials for creating the optical ladder.

riches the quantum states. For example, a phase separation between superfluid and normal phases was observed in attractively interacting ultracold Fermi atoms [14, 15]. On the other hand, a magnetic structure with spin imbalance in repulsively interacting fermionic atoms with and without OLs has been studied in a weak-correlation regime [8–10].

The reason why we take the ladder is as follows. The long history of itinerant ferromagnetism has made us realize that Stoner's picture is mean-field theoretic, while almost the only model in which itinerant ferromagnetism can be rigorously shown is Nagaoka's ferromagnetism, which requires rather a pathological (infinitely strong interaction and an infinitesimal doping in a half-filled band) limit [16]. The Nagaoka ferromagnetism has yet to be experimentally confirmed, although von Stecher *et al.* recently proposes a way to realize the Nagaoka ferromagnetism in optical plaquette systems with the high

* okumura@riken.jp

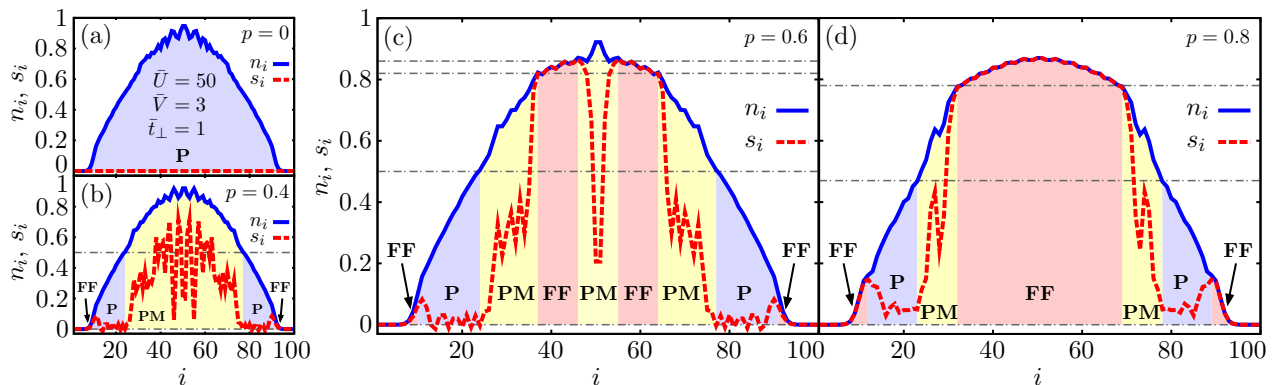


FIG. 2. (Color online) The particle density (n_i ; blue solid line) and spin density (s_i ; red dashed line) for the spin polarization $p = 0$ (a), 0.4 (b), 0.6 (c), and 0.8 (d) with $\bar{U} = 50$, $\bar{V} = 3$, $\bar{t}_\perp = 1$, and $L = 100$. P, PM, and FF denote paramagnetic, partially magnetic, and fully ferromagnetic states, respectively. The dash-dotted lines represent the n_i at numerically obtained phase boundaries.

tunability of OL system [11]. On the other hand, some theories indicate that the two-leg ladder can realize an itinerant ferromagnetism that accommodates finite interaction and finite doping, which is connected to Nagaoka's in the limit of $U \rightarrow \infty$ or large inter-leg transfer [17, 18]. Experimentally, an optical ladder may be created by a superposition of normal lattice potential (along x) and super-lattice potential (y) (Fig. 1). This should be realizable because a superlattice potential has been used in the experiments with bosonic atoms [3, 19]. To confine the atoms we impose a trapping potential as well, and we explore the ground states in this situation. We want to treat very strong repulsive interactions, but the system, being quasi-one dimensional, can be treated with the density-matrix renormalization-group (DMRG) method [20, 21], which can also treat effects of the trapping potential [22]. We show that an itinerant ferromagnetism does appear in an optical ladder with an interesting phase separation between a fully-polarized ferromagnetic domain originating from the extended Nagaoka mechanism with finite hole density. This ground state should be easily observed by *in situ* imaging method [14], which is the main reason why we consider the spin-imbalance. In addition, we find the enhancement of the formation of the finite hole-density Nagaoka ferromagnetism by the spin-imbalance.

Formulation — We take the simplest possible repulsive Hubbard model on a ladder in a trapping potential applied along the leg. The Hamiltonian then reads, in the standard notation,

$$\hat{\mathcal{H}} = -t \sum_{\langle i,j \rangle, \alpha, \sigma} \hat{c}_{i\sigma}^{\alpha\dagger} \hat{c}_{j\sigma}^\alpha - t_\perp \sum_{i, (\alpha, \beta), \sigma} \hat{c}_{i\sigma}^{\alpha\dagger} \hat{c}_{i\sigma}^\beta + U \sum_{i, \alpha} \hat{n}_{i\uparrow}^\alpha \hat{n}_{i\downarrow}^\alpha + V \sum_{i, \alpha, \sigma} (i - x_c)^2 \hat{n}_{i\sigma}^\alpha, \quad (1)$$

where, $i, j = 1, 2, \dots, L$ (L : the ladder length) label the sites along the legs with $\langle i, j \rangle$ being nearest-neighbor sites connected by a hopping integral t , $\alpha = 1, 2$ labels the sites

along the rungs with t_\perp being the hopping along the rung. $U (\geq 0)$ is the repulsive, on-site interaction [23], while V is the strength of the trapping potential, which is assumed to be harmonic around the center, $x_c = (L+1)/2$ with the lattice constant taken to be unity. It should be mentioned that the maximum value of \bar{U} for stable Hubbard model in the current experiment is 180 [4]. We assume that the harmonic confinement along the rung (superlattice) direction is very weak. In addition, we also assume that the inter-ladder hoppings are negligible.

The total spin imbalance is defined as $p = (N_\uparrow - N_\downarrow)/N$, where $N_\sigma = \sum_{i, \alpha} \langle \hat{n}_{i\sigma}^\alpha \rangle$ and $N = \sum_\sigma N_\sigma$, and $\langle \cdot \rangle$ represents the expectation value. All the numerical results respect the symmetry, $\langle \hat{n}_{i\sigma}^1 \rangle = \langle \hat{n}_{i\sigma}^2 \rangle$, so that we can introduce the rung particle density $n_i = \langle \hat{n}_{i\uparrow}^1 \rangle + \langle \hat{n}_{i\downarrow}^1 \rangle$, and the rung spin density $s_i \equiv \langle \hat{n}_{i\uparrow}^1 \rangle - \langle \hat{n}_{i\downarrow}^1 \rangle$. For convenience, we use dimensionless parameters as $\bar{t}_\perp = t_\perp/t$, $\bar{U} \equiv U/t$, and $\bar{V} \equiv V/t \times 10^3$. In this paper, we fix the total number of atoms as $N = 100$ with the length of the ladder $80 \leq L \leq 180$. The number, m , of the states retained in the present DMRG calculations is 800–1200, which are numerically shown to give converged results.

DMRG results — Let us show the DMRG results. Figure 2 shows profiles of n_i and s_i in the ground states for various p in a strongly-interacting case ($\bar{U} = 50$) with $\bar{t}_\perp = 1$ and $\bar{V} = 3$. In the spin-balanced case ($p = 0$) [Fig.2(a)], a paramagnetic (P) phase appears. As we increase p to 0.4 , a partially magnetic (PM) phase starts to appear in the middle of the system [Fig. 2(b)]. If we further increase p to 0.6 , fully ferromagnetic (FF) regions emerge in the ground state [Fig. 2(c)] in a more complex phase-separated structure. For $p = 0.8$, the FF region covers almost the whole system, sandwiched by narrow PM and P regions [Fig. 2(d)].

In order to demonstrate both of the effect of strong interaction and the effect of the ladder configuration (a connectivity condition [16]) are at work for realization of the FF phases in the regions with $0.8 < n < 0.9$, we compare the result with the one in a weakly-interacting case with

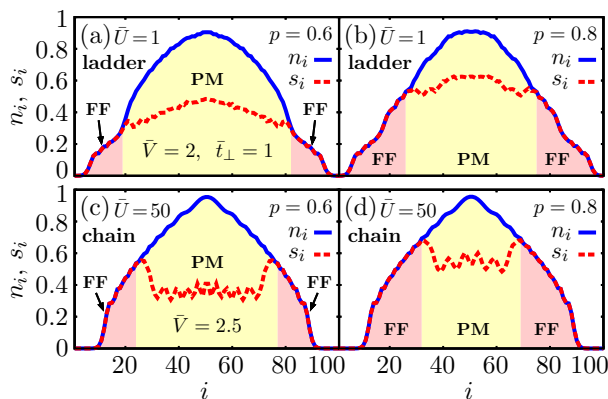


FIG. 3. (Color online) The particle density n_i (blue solid lines) and spin density s_i (red dashed lines) for a weakly-interacting ladder system ($\bar{U} = 1$, $\bar{V} = 2$, $\bar{t}_\perp = 1$, and $L = 100$) with $p = 0.6$ (a) or 0.8 (b), and for a strongly-interacting single chain ($\bar{U} = 50$ and $\bar{V} = 2.5$) with $p = 0.6$ (c) or 0.8 (d) for $N = 50$.

connectivity [two-leg ladder, $\bar{U} = 1$, $\bar{V} = 2$, and $\bar{t}_\perp = 1$; Figs. 3(a)(b)], and with the one in a strong-interacting case without connectivity [single chain, $\bar{U} = 50$, and $\bar{V} = 2.5$; Figs. 3(c)(d)]. We can immediately see that FF phases do not emerge in these systems, although there are narrow FF regions around the edges. This clearly indicates that the FF phases with $0.8 < n < 0.9$ in the ladder arise due to a combined effect of the strong interaction and the connectivity condition, i.e., the finite hole-density Nagaoka ferromagnetism [17].

Now, the question is what determines the spatial distribution of majority and minority spins as the spin imbalance is increased. As a key, we can examine the energy gap, $\Delta\bar{E} = (E_{S_z=0} - E_{S_z=N/2})/Lt$, of the FF above the lowest energy of the nonmagnetic state in the uniform system ($V = 0$), as in the t - J model in [17] but here for the Hubbard model. The gap depends on the particle density n as depicted in Fig. 4. As U is increased the curve approaches the $\Delta\bar{E} = 0$ axis around $n \sim 0.8$, which means that the ferromagnetic phase becomes closer to the ground state. Such a non-trivial structure is naturally absent in the single-chain Hubbard model, as shown in the inset of the figure.

With this picture we can interpret the results shown in Figs. 2, 3(c) and 3(d). When the trapping potential is not too strong so that the spatial variation of the density is slow, we can locally define the energy gap as given in Fig. 4. The energy gap and the trapping potential determine the phase separation: Let us first look at the strongly interacting 1D chain, both of the majority ($= (n_i + s_i)/2$) and minority ($= (n_i - s_i)/2$) spins are accumulated in the middle where $n \simeq 1$ [Figs. 3(c)(d)]. Non-FF states are preferred because both of $\Delta\bar{E}(n)$ (Fig. 4, inset) and the trapping potential favor $n \simeq 1$, which is a realization of the Lieb-Mattis theorem [24]. This leads us to a natural interpretation that the ground-state energy is lowered by gathering minority spins around the

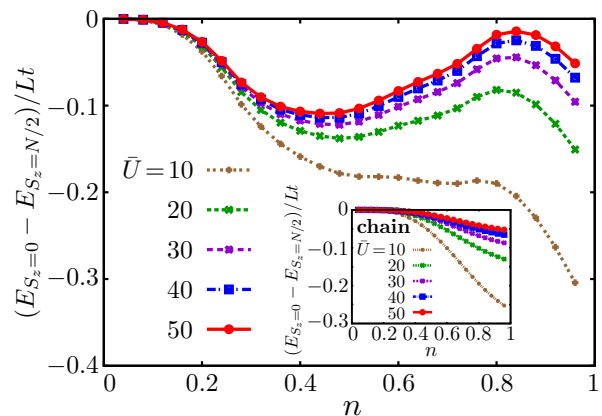


FIG. 4. (Color online) The density dependence of the energy gap $\Delta\bar{E} = (E_{S_z=0} - E_{S_z=N/2})/Lt$ in homogeneous systems ($\bar{V} = 0$) with $\bar{t}_\perp = 1$ for various values of U . The inset is the same plot for the homogeneous single chain. Here the parameters are $L = 50$, $\bar{t}_\perp = 1$ and $m = 1200$ (ladder) or $m = 1000$ (chain).

trap center to construct an antiferromagnetic correlation. On the other hand, in a strongly-interacting ladder, we obtain the ferromagnetic region, which may seem counterintuitive, but is in fact viewed as a manifestation of the extended Nagaoka mechanism [17]. Namely, the minority spins in Fig. 2(d) reside in the regions with relatively high potential energy ($i < 31$ and $70 < i$), but this is compensated by a large energy $\Delta\bar{E}$ gained by forming the non-FF state (Fig. 4). Conversely, FF state is stabilized for $0.8 < n < 0.9$, where $\Delta\bar{E}$ is small. Hence the phase separation arises. By contrast, the phase separation seen for a weak U in the ladder in Figs. 3 (a)(b) has a simple origin, i.e., both majorities and minorities are accumulated by the trapping potential and form doubly occupied states because the inter-particle interaction is weak. Finally, the spin-imbalance enhances the formation of the finite hole-density Nagaoka ferromagnetism, i.e., the FF regions with $0.8 < n < 0.9$ appear when $p = 0.6$ and 0.8 [Figs. 2(c)(d)], although they disappear in the spin-balanced case [Fig. 2(a)] due to a small gap $\Delta\bar{E}$ around $n \sim 0.8$ (Fig. 4) [25].

Phase diagram — Having clarified the mechanism for the phase-separated magnetism, we now explore a phase diagram against \bar{U} , \bar{V} , and \bar{t}_\perp . First, we focus on the dependence on \bar{V} and \bar{U} for $p = 0.8$ with $\bar{t}_\perp = 1$ in Figs. 5(a). We characterize the FF region by \tilde{N}_{FF} , which is the number of sites having $n_i = s_i$ within 10^{-2} normalized by the maximum value of this quantity. We find that there is optimum $\bar{U} \simeq 50$ and $\bar{V} \simeq 3$ to make \tilde{N}_{FF} maximum. To trace back how the optimum \bar{U} and \bar{V} arise, we can look at n_i and s_i plotted for various values of \bar{V} and \bar{U} in Figs. 5(b)-(d). If we first combine Figs. 2(d), 5(b)(d) for the effect of varied \bar{V} with a fixed $\bar{U} = 50$, we can see that the central FF region broadens when \bar{V} increases from 1 to 3 [Figs. 2(d), 5(b)] because the region with $n_i > 0.8$ becomes wider with \bar{V} . If the trap becomes

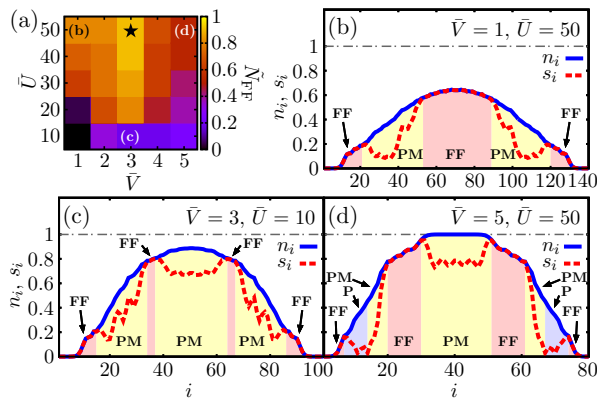


FIG. 5. (Color online) (a) \tilde{N}_{FF} plotted against \tilde{V} and \tilde{U} for $\bar{t}_{\perp} = 1$ and $p = 0.8$. In the color-coding \tilde{N}_{FF} is normalized by the maximum [a star at $\tilde{V} = 3, \tilde{U} = 50$, which corresponds to Fig. 2(d)] in the parameter region considered. Also plotted are n_i (blue solid lines) and s_i (red dashed) with $(\tilde{V}, \tilde{U}) = (1, 50)$ (b), $(5, 50)$ (c), and $(3, 10)$ (d).

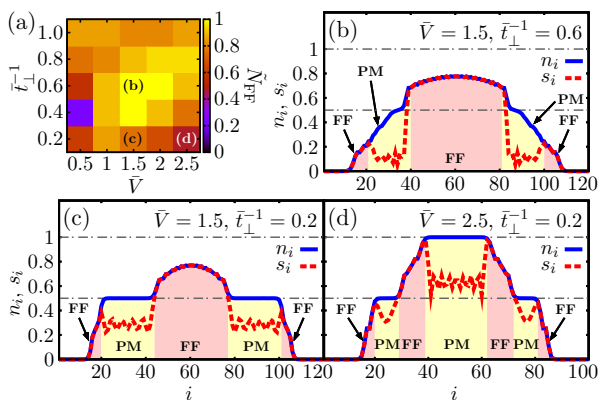


FIG. 6. (Color online) (a) Color-coded \tilde{N}_{FF} against \tilde{V} and \bar{t}_{\perp}^{-1} for $\tilde{U} = 50$ and $p = 0.8$. Also plotted are n_i (blue solid lines) and s_i (red dashed) with $(\tilde{V}, \bar{t}_{\perp}^{-1}) = (1.5, 0.6)$ (b), $(1.5, 0.2)$ (c), $(2.5, 0.2)$ (d).

too strong in Fig. 5(d), however, the FF region gives way to the PM Mott plateau because n_i reaches 1. If we turn

to dependence on the interaction strength, we can look at the results for $\tilde{U} = 10-50$ with a fixed $\tilde{V} = 3$ [Figs. 2(d), 5(c)]. As the interaction is decreased to 10 in Fig. 5(c) the FF region shrinks, where the reason should be that $\Delta\bar{E}$ becomes large at $n \sim 0.8$ when \tilde{U} is as small as 10.

Finally we consider the effect of \bar{t}_{\perp} . A phase diagram in terms of \tilde{N}_{FF} , against \tilde{V} and \bar{t}_{\perp}^{-1} this time, is displayed in Fig. 6(a). We find that a finite \bar{t}_{\perp} is suitable for largest \tilde{N}_{FF} in this figure, which is contrast to the homogeneous system in which the infinite \bar{t}_{\perp} is best. The reason is that a charge gap opens at $n_i = 0.5$ [17], at which the FF phase gives way to the insulating state when \bar{t}_{\perp}^{-1} is small [Figs. 6(b)–(d)]. This degrades the FF phase stability.

Summary — We have found for spin-imbalanced and strongly repulsive-interacting Fermi atoms on an optical ladder that ferromagnetic regions appear in a phase-separated structures. Their emergence is caused by a combined effect of the strong interaction and the connectivity condition, i.e., the extended Nagaoka mechanism. The origin of the phase separation is explained by the density dependence of the energy gap between fully spin-polarized and other states in homogeneous system. As for finite temperatures, it was shown, with the dynamical mean-field theory, that the finite hole-density Nagaoka ferromagnetism is robust against thermal fluctuations in two-dimensional system [26]. Then we expect the phase separation is also robust at finite temperatures. Another future problem is how the itinerant ferromagnetism treated here in the spin-imbalanced condition would be related to the balanced case. Along the line, a study of correlation functions in spin-balanced case is under way [25], where we observe phase separation between non-magnetic and ferromagnetic (for the S_x and S_y direction) phases. We can however emphasize that the phase separation involving the FF regions for the S_z direction will be easier to be observed with *in situ* imaging methods [14] than the correlation functions.

One of authors (M.O.) wishes to thank R. Igarashi, N. Nakai, H. Nakamura, and Y. Ota for fruitful discussion. The work was partially supported by Grant-in-Aid for Scientific Research (20500044) from MEXT, Japan.

[1] For a recent review, see, e.g., I. Bloch, J. Dalibard, and W. Zwerger, *Rev. Mod. Phys.* **80**, 885 (2008).
 [2] For a recent review, see, e.g., M. Lewenstein *et al.*, *Adv. Phys.* **56**, 243 (2007), and references therein.
 [3] S. Trotzky *et al.*, *Science* **319**, 295 (2008).
 [4] R. Jördens *et al.*, *Nature (London)* **455**, 204 (2008).
 [5] U. Schneider *et al.*, *Science* **322**, 1520 (2008).
 [6] L. Salasnich *et al.*, *J. Phys. B* **33**, 3943 (2000); T. Sogo and H. Yabu, *Phys. Rev. A* **66**, 043611 (2002); R.A. Duine and A.H. MacDonald, *Phys. Rev. Lett.* **95**, 230403 (2005); I. Berdnikov, P. Coleman, and S.H. Simon, *Phys. Rev. B* **79**, 224403 (2009); H. Zhai, *Phys. Rev. A* **80**, 051605(R) (2009); G.J. Conduit and B.D. Si-

mons, *Phys. Rev. Lett.* **103**, 200403 (2009); G.J. Conduit, A.G. Green, and B.D. Simons, *ibid* **103**, 207201 (2009); S. Pilati *et al.*, *ibid* **105**, 030405 (2010); X. Cui and H. Zhai, *Phys. Rev. A* **81**, 041602(R) (2010).
 [7] L. Wang *et al.*, *Phys. Rev. A* **78**, 023603 (2008); K. Noda *et al.*, *ibid* **80**, 063622 (2009); S. Zhang, H. Hung, and C. Wu, *ibid* **82**, 053618 (2010).
 [8] G.J. Conduit and B.D. Simons, *Phys. Rev. A* **79**, 053606 (2009).
 [9] L.J. LeBlanc, J.H. Thywissen, A.A. Burkov, and A. Paramekanti, *Phys. Rev. A* **80**, 013607 (2009).
 [10] B. Wunsch *et al.*, *Phys. Rev. A* **81**, 013616 (2010).
 [11] J. von Stecher *et al.*, *New J. Phys.* **12**, 055009 (2010).

- [12] G.-B. Jo *et al.*, *Science* **325**, 1521 (2009).
- [13] D. Pekker *et al.*, *Phys. Rev. Lett.* **106**, 050402 (2011).
- [14] M.W. Zwierlein *et al.*, *Nature (London)* **442**, 54 (2006); M.W. Zwierlein *et al.*, *Science* **311**, 492 (2006); Y. Shin *et al.*, *Phys. Rev. Lett.* **97**, 030401 (2006).
- [15] G.B. Partridge *et al.*, *Science* **311**, 503 (2006); G.B. Partridge *et al.*, *Phys. Rev. Lett.* **97**, 190407 (2006).
- [16] Y. Nagaoka, *Phys. Rev. B* **147**, 392 (1966); D.J. Thouless, *Proc. Phys. Soc. London* **86**, 893 (1965); H. Tasaki, *Phys. Rev. B* **40**, 9192 (1989).
- [17] M. Kohno, *Phys. Rev. B* **56**, 15015 (1997).
- [18] R. Arita *et al.*, *Phys. Rev. B* **58**, R11833 (1998).
- [19] J. Sebby-Strabley *et al.*, *Phys. Rev. A* **73**, 033605 (2006).
- [20] S. R. White, *Phys. Rev. Lett.* **69**, 2863 (1992); *Phys. Rev. B* **48**, 10345 (1993).
- [21] For recent reviews, see e.g., U. Schollwöck, *Rev. Mod. Phys.* **77**, 259 (2005); K. A. Hallberg, *Adv. Phys.* **55**, 477 (2006), and references therein.
- [22] Specifically, the directly-extended DMRG method [S. Yamada, M. Okumura, and M. Machida, *J. Phys. Soc. Jpn.* **78**, 094004 (2009)] developed by three of the present authors is used to obtain accurate results in this system.
- [23] The on-site interaction parameter is given by $U = 4\sqrt{\pi}(a/a_{\text{lat}})E_r[(4V_s + V_l)/E_r]^{1/4}(4V_s/E_r)^{1/4}(V_z/E_r)^{1/4}$ ($V_0 \gg E_r$) for the periodic OL potential $V(\mathbf{r}) = V_s \sin^2(2kx) + V_l \sin^2(kx) + V_s \sin^2(2ky) + V_z \sin^2(kz)$, where a_{lat} is the lattice constant of the long-period potential, V_s , V_l , and V_z the depths of the short-period, long-period and z -direction potentials, respectively, and $E_r = 4\pi^2\hbar^2/2ma_{\text{lat}}^2$ the recoil energy [1].
- [24] E.H. Lieb and D.C. Mattis. *Phys. Rev.* **125**, 164 (1962); B. Kumar, *Phys. Rev. B* **79**, 155121 (2009).
- [25] M. Okumura, S. Yamada, M. Machida, and H. Aoki, unpublished.
- [26] H. Park *et al.*, *Phys. Rev. B* **77**, 035107 (2008).